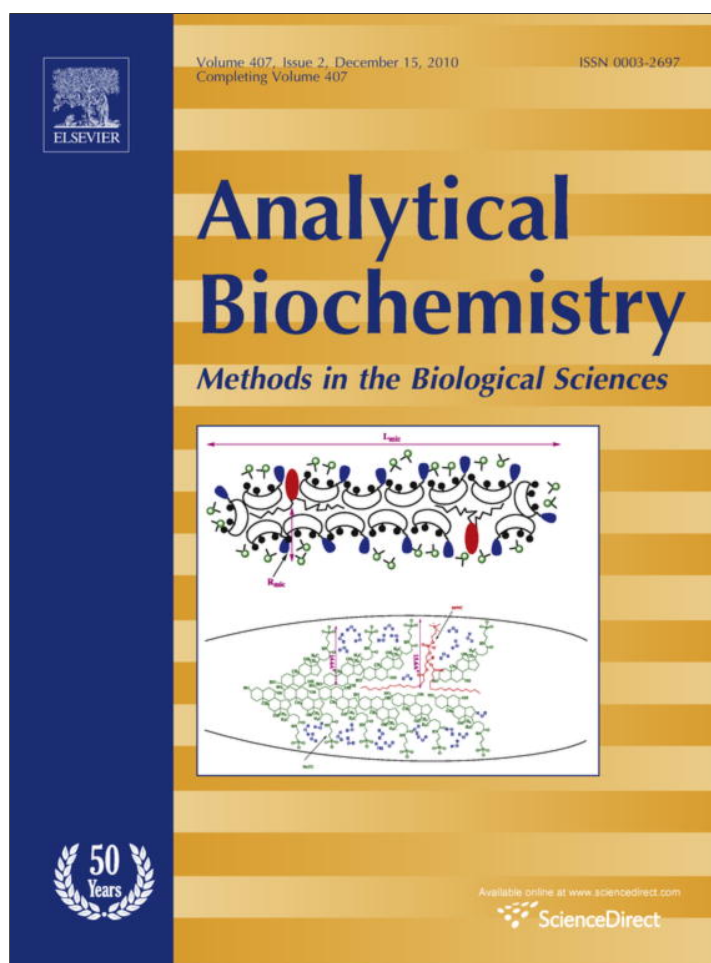


Provided for non-commercial research and education use.
Not for reproduction, distribution or commercial use.



This article appeared in a journal published by Elsevier. The attached copy is furnished to the author for internal non-commercial research and education use, including for instruction at the authors institution and sharing with colleagues.

Other uses, including reproduction and distribution, or selling or licensing copies, or posting to personal, institutional or third party websites are prohibited.

In most cases authors are permitted to post their version of the article (e.g. in Word or Tex form) to their personal website or institutional repository. Authors requiring further information regarding Elsevier's archiving and manuscript policies are encouraged to visit:

<http://www.elsevier.com/copyright>



Contents lists available at ScienceDirect

Analytical Biochemistry

journal homepage: www.elsevier.com/locate/yabio

Trace detection of picloram using an electrochemical immunosensor based on three-dimensional gold nanoclusters

Lijuan Chen, Guangming Zeng*, Yi Zhang, Lin Tang, Danlian Huang, Can Liu, Ya Pang, Jie Luo

College of Environmental Science and Engineering, Hunan University, Changsha 410082, China

Key Laboratory of Environmental Biology and Pollution Control (Hunan University), Ministry of Education, Changsha 410082, China

ARTICLE INFO

Article history:

Received 23 April 2010

Received in revised form 1 August 2010

Accepted 2 August 2010

Available online 13 August 2010

Keywords:

Picloram

3D Au nanoclusters

Horseradish peroxidase

Electrochemical immunosensor

ABSTRACT

Picloram, a herbicide widely used for broadleaf weed control, is persistent and mobile in soil and water with adverse health and environmental effects. It is important to develop a sensitive method for accurate detection of trace picloram in the environment. In this article, a type of ordered three-dimensional (3D) gold (Au) nanoclusters obtained by two-step electrodeposition using the spatial obstruction/direction of the polycarbonate membrane is reported. Bovine serum albumin (BSA)-picloram was immobilized on the 3D Au nanoclusters by self-assembly, and then competitive immunoreaction with picloram antibody and target picloram was executed. The horseradish peroxidase (HRP)-labeled secondary antibody was applied for enzyme-amplified amperometric measurement. The electrodeposited Au nanoclusters built direct electrical contact and immobilization interface with protein molecules without postmodification and positioning. Under the optimal conditions, the linear range for picloram determination was 0.001–10 µg/ml with a correlation coefficient of 0.996. The detection and quantification limits were 5.0×10^{-4} and 0.0021 µg/ml, respectively. Picloram concentrations in peach and excess sludge supernatant extracts were tested by the proposed immunosensor, which exhibited good precision, sensitivity, selectivity, and storage stability.

Crown Copyright © 2010 Published by Elsevier Inc. All rights reserved.

Chlorinated pesticides have been used in agricultural production and rangeland improvements to prevent and control plant diseases and insect pests for more than 50 years [1]. They are refractory and persistent in environment, can accumulate in the human body through the food chain, and become the potential pathogenic factors [2]. Although they have been forbidden or restricted to use in many countries, some of them are still frequently used for pest or weed control. Picloram (4-amino-3,5,6-trichloro-2-pyridinecarboxylic acid) is a herbicide used for broadleaf weed control in pasture and rangeland, wheat, barley, oats, and woody plant species [3]. It acts as a plant growth regulator, mimicking naturally occurring plant auxins or the hormone indoleacetic acid and inhibiting the synthesis of proteins [4]. Picloram is highly water soluble (430 mg/l) and moderately or highly persistent in the soil environment, with reported field half-lives from 20 to 300 days and an estimated average of 90 days [5]. As a result of agricultural application and improper waste disposal, it might leach into surface and ground waters, move from treated plants to damage nearby nontarget crops, and pose toxic hazard to aquatic species at µg/ml concentrations [6]. Recent research has indicated that picloram is one type of environmental hormone with

low toxicity but carcinogenicity. High levels of the herbicide can damage the human central nervous system and reproductive system to a certain extent or cause other health problems [7]. According to the U.S. Environmental Protection Agency, the maximum contaminant level for picloram in drinking water is 0.5 µg/ml [8]. To reduce the risk of these adverse health effects, picloram must be controlled at low concentration in the environment. Therefore, a simple and reliable detection method is needed.

Currently, gas/liquid chromatography with electron capture detector and capillary electrophoresis/mass spectrometry are the common methods for detection and quantification of picloram. They have lower limits of detection (LODs)¹ and are extremely sensitive, but they frequently involve extensive sample extraction and purification procedures and require well-equipped laboratory installations [9,10]. Enzyme-linked immunosorbent assays (ELISAs) and radioimmunoassays (RIAs) have been proved to be effective methods for picloram detection [11–13], but the complicated

* Corresponding author at: College of Environmental Science and Engineering, Hunan University, Changsha 410082, China. Fax: +86 731 88823701.

E-mail address: zgming@hnu.cn (G. Zeng).

¹ Abbreviations used: LOD, limit of detection; ELISA, enzyme-linked immunosorbent assay; RIA, radioimmunoassay; Au, gold; Pt, platinum; 3D, three-dimensional; GCE, glassy carbon electrode; PC, polycarbonate; BSA, bovine serum albumin; HRP-G anti-RlgG, horseradish peroxidase-labeled goat anti-rabbit immunoglobulin G; PBS, phosphate buffer solution; SCE, saturated calomel electrode; SEM, scanning electron micrograph; CV, cyclic voltammetry; DMF, dimethylformamide; EIS, electrochemical impedance spectroscopy; LOQ, limit of quantification.

washing procedure and long incubation time, or radiation hazards and large instruments, limit their application in on-site pesticide control. Therefore, a more convenient and economical method is needed. An electrochemical immunosensor can overcome many of the difficulties described above and provide a fast, on-site, and fully automated detection method of environmental samples without pretreatment [14–16].

Nowadays, nanomaterials-based electrochemical immunoassays have attracted considerable interest due to their special physical, chemical, and mechanical properties. Many types of nanomaterials, such as Fe₃O₄ magnetic nanoparticles [17,18], gold (Au)–platinum (Pt) bimetallic nanoparticles [19], CdS nanoparticles [20], Ag nanoparticles [21], and Pd nanoparticles [22], have been developed. Au nanoparticle is a popular material in related fields due to easy synthesis and excellent electrical, mechanical, and optical properties [23–25]. In addition, Au nanoparticles can offer a large specific surface, promote the electron transfer, and retain the bioactivity of immobilized biomolecules. In Furthermore, the three-dimensional (3D)-structure nanoparticles are especially superior and have been employed for modifying sensor electrode surface to immobilize biomolecules [26,27]. Many methods to synthesize 3D nanostructure on electrode surface have been reported, including microfabrication [28], breath figures on conducting polymers [29], electrochemical synthesis of conducting polymers in the presence of surfactant [30], chemical vapor deposition [31], and plasma etching of metal-filled membranes [32]. A general method for fabricating 3D nanostructure is template synthesis, during which the metal particles are grown within the cylindrical and monodisperse pores of nanoporous membrane by electroless deposition.

In this study, the 3D Au nanocluster was synthesized to modify the glassy carbon electrode (GCE) for the detection of picloram in peach and excess sludge supernatant. According to Wang et al. [33], to fabricate 3D Au nanocluster using porous polycarbonate (PC) membrane with little modification, a more stable intact nanocluster was obtained. Based on the 3D nanostructure, an electrochemical immunosensor was developed to detect picloram using competitive immunoreaction. Bovine serum albumin (BSA)–picloram was immobilized on the 3D Au nanoclusters and then competed with target picloram to react with picloram antibody. Horseradish peroxidase-labeled goat anti-rabbit immunoglobulin G (HRP-G anti-RlgG) would provide detectable signal. This system shows high sensitivity and a low LOD in picloram detection. To the best of our knowledge, this is the first time the two-step method has been used to synthesize 3D Au nanoclusters that modified GCE for picloram detection.

Materials and methods

Reagents and apparatus

The analytical standards of picloram, clopyralid, fluroxypyr methyl, quinclorac, and lontrel were purchased from J&K Chemical (Beijing, China). HRP-G anti-RlgG was obtained from Dingguo Biotechnology (Beijing, China). Nonfat dried milk was obtained from Jiehui Biotechnology (Changsha, China). BSA–picloram and picloram antibody were home-synthesized [16]. All other chemicals were of analytical grade, and all solutions were prepared in deionized water of 18 M Ω purified from a Milli-Q purification system. Phosphate buffer solution (PBS) with 0.01 mol/L NaH₂PO₄ and 0.01 mol/L Na₂HPO₄ was used in this work.

Electrochemical measurements were carried out on a CHI660B electrochemistry system (Chenhua Instrument, Shanghai, China). The three-electrode system used in this work consisted of a GCE (diameter of 3 mm) as working electrode of interest, a saturated calomel electrode (SCE) as reference electrode, and a Pt foil auxil-

iary electrode. All work was performed at room temperature (25 °C) unless otherwise mentioned. Track-etched porous PC (0.2 μ m) membrane was provided by Whatman. Scanning electron micrographs (SEMs) of the membranes were obtained with a JSM-6700F field emission scanning electron microscope (JEOL, Japan). A model PHSJ-3F laboratory pH meter (Leici Instrument, Shanghai, China) was used to test pH values. In amperometric measurement, a magnetic stirrer was used to stir the solution. A 4K15 Sigma centrifuge (Sartorius, Germany) was used in the assay.

Electrodepositing Au nanoprickle clusters on GCE

The GCE was first polished thoroughly with 0.5 mm alumina paste; sonicated in 1:1 (v/v) HNO₃, acetone, and water successively; and rinsed with water before use. The electrodeposition was divided into two steps. First, the GCE was dipped into 1% (w/w) HAuCl₄ solution containing 0.5 M perchloric acid and deposited at a potential of 0.2 V for 50 s. Second, the GCE was taken out and maintained in the air until the surface was dry. Then a PC template was carefully attached on the surface and fixed by a rubber O-ring. Deposition of this step was operated in the same solution but at a potential of 0.18 V for 300 s. After that, the PC template was dissolved by immersing the electrode in chloroform. Having been rinsed with water thoroughly, the obtained electrode was ready for the immune procedure.

Preparing picloram immunosensor

Scheme 1 is a schematic diagram of the immunosensor based on competitive immunoreaction. The nanoclusters deposited on GCE were covered by 15 mg/ml BSA–picloram for 2 h. Nonfat dried milk (3%) was used to block the nonspecific binding sites of the electrode. Next the electrode was soaked in 300 μ l of various concentrations of picloram solutions containing certain picloram antibody for 1 h. The immobilized BSA–picloram and the target picloram would compete to react with picloram antibody. Then the electrode was covered by 10 μ l of HRP-G anti-RlgG diluted with PBS (pH 7.6) for 40 min. The electrode was rinsed with PBS after each step, and the incubation procedure was performed at 37 °C.

Electrochemical measurements

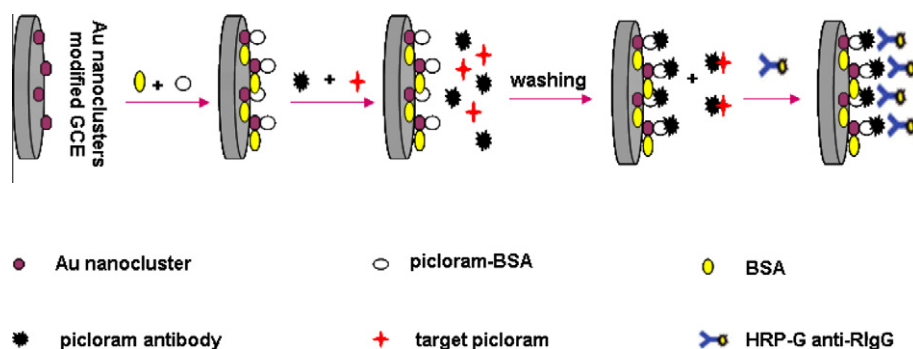
Alternating current impedance behavior was obtained in 5 mM K₃[Fe(CN)₆]/K₄[Fe(CN)₆] containing 0.1 M KCl, and the frequency ranged from 1 to 100,000 Hz with an AC amplitude of \pm 5 mV. Cyclic voltammetry (CV) was performed in 0.01 M PBS (pH 7.4) containing 1 mM hydroquinone and 2 mM H₂O₂, with a potential range from –0.4 to +0.8 V versus SCE at 100 mV/s. The chronoamperometry was carried out in the same electrolyte at the potential of –0.2 V under increasing stirring. The current changes reflected the catalytic activity of the HRP. The reduction current was recorded as I_x . When no picloram existed in the competitive immunoreaction, the reduction current was recorded as I_0 . The decreased percentage (DP) of current is given by

$$DP = \frac{I_0 - I_x}{I_0} \times 100.$$

After each immunoassay and detection, the immunosensor was regenerated and prepared for the next detection.

Extraction of picloram from samples

Put into a flask were 6 g of peach chopped in fine pieces and 20 ml of MeOH, and the flask was shaken at 37 °C for 3 h on a mechanical vibrator at 120 rpm. Then the solution was filtered. The container and the residue were rinsed with 10 ml of MeOH and filtered, and



Scheme 1. Schematic diagram of the immunosensor based on competitive immunoreaction.

the filtrate was combined with the previous filtrate. The filtrate was diluted, and the pH value was adjusted to 7.4 with the PBS.

The excess sludge was centrifuged at 4000 rpm for 10 min, and then the supernate was filtered. The filtrate was adjusted to pH 7.4 with the PBS.

The prepared samples were spiked with different concentration of picloram separately and stored at 4 °C.

Regeneration of biosensor

When the immunoassay procedures were over, the electrode was regenerated by rinsing consecutively in 0.2 M NaOH solution containing 0.5 M NaCl for 10 min and then in dimethylformamide (DMF) for 20 min. The resulting electrode was ready for the next immunoassay.

Results and discussion

Characterization of Au nanoclusters

Fig. 1 is the SEM image of the Au nanoclusters of the two-step deposition. Fig. 1A shows the low-magnification image of the first

step deposition. The Au nanoclusters dispersed densely on the electrode surface with nonuniform size. However, the nanocluster morpha can be seen clearly in the high-magnification image (Fig. 1B). The nanocluster looks like a pellet with some prickles around it, and its average diameter was approximately 300 nm. After the second step deposition, the nanoclusters were densified and changed uniformly in a low-magnification image (Fig. 1C). The nanoclusters were turned into a multisheet columnar structure in high-magnification image, and the average diameter increased slightly to 500 nm (Fig. 1D), with each columnar structure consisting of thin slices with a diameter of 200 nm.

The two-step electrodeposition of Au nanoclusters was different from the one-step deposition. The nanoparticles by one-step deposition fell off easily during the PC membrane dissolution process. To improve the fixing, a thin layer of Au nanoparticles was deposited directly on the electrode surface at first. The first deposited Au nanoparticles were “seeds” that acted as catalysts for the reduction of AuCl₄⁻. The Au nanoparticles formed in the first step could guide the growth of Au nanoparticles in the second step, and then Au nanocluster stability was improved.

We supposed that these Au nanoclusters grew up along the channel of the PC membrane pores for orientation. The columnar

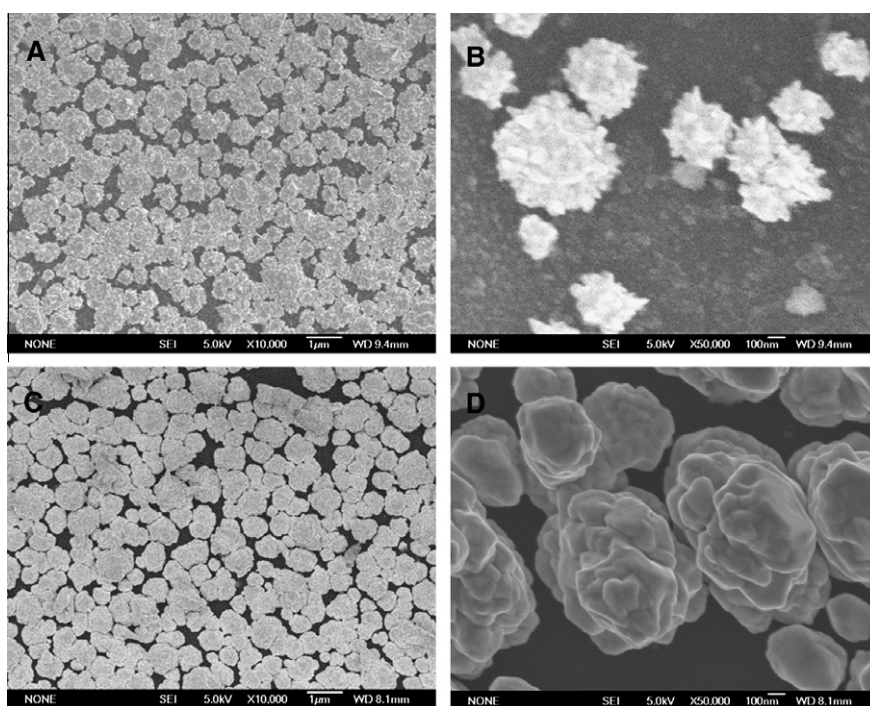


Fig. 1. Typical SEM images of Au nanoclusters: (A) low-magnification image of the first step deposition; (B) high-magnification image of the first step deposition; (C) low-magnification image of the second step deposition; (D) high-magnification image of the second step deposition.

structure significantly increased the specific surface area of each cluster, and this was effective for biomolecule immobilization. In addition, the Au nanoclusters on the electrode surface could remarkably facilitate the electron transfer. The great specific surface area of Au nanoclusters and their enhanced electron transfer capability could offer more response sites and cause a fast amperometric response.

Preparation of picloram immunosensor and immunoassay

Electrochemical impedance spectroscopy (EIS) was carried out in a background solution of 5 mM $K_3Fe(CN)_6/K_4Fe(CN)_6$ in the presence of 0.1 M KCl to investigate the features of surface-modified electrode. The Au nanoclusters, BSA–picloram, picloram antibody, and HRP–G anti-RlgG were successively modified onto the GCE and measured. The typical impedance spectrum (present in the form of a Nyquist plot) includes a semicircle portion at higher frequency corresponding to the electron transfer limiting process and a linear part at a lower frequency range representing the diffusion limiting process. The semicircle diameter in the impedance spectrum equals the electron transfer resistance, R_{ct} , which shows its blocking behavior for the redox couple. Thus, the diameter can be used to describe the resistance interface properties of the electrode, and its increasing value exactly characterizes the immobilization for each step.

Fig. 2 shows the Nyquist plot of electrochemical impedance spectra for the stepwise assembly. The electron transfer resistance gradually increased with the assembly procedure. The Au nanoclusters modified electrode exhibited a nearly straight line (curve a), which showed good electron transfer capability. After BSA–picloram was immobilized onto the electrode, the semicircle diameter increased remarkably (curve b). We supposed that a large amount of BSA–picloram was immobilized on the binding sites in the Au nanoclusters. When picloram antibody was added, the diameter of the semicircle increased further (curve c), indicating that the immunoreaction had finished. The transfer resistance sequentially increased with the introduction of the HRP–G anti-RlgG onto the electrode surface (curve d). The correspondingly increasing resistance indicated that the construction of the immunosensor was feasible.

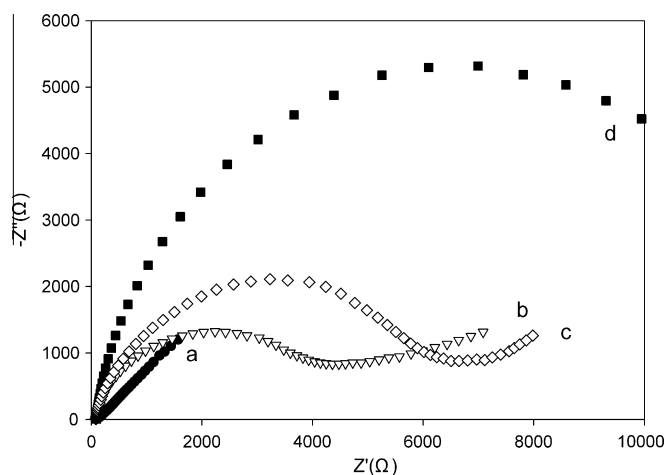


Fig. 2. Nyquist diagrams of electrochemical impedance at different stages: (a) GCE electrode modified with Au nanoclusters; (b) BSA–picloram immobilized electrode; (c) BSA–picloram immobilized electrode exposed to picloram antibody solution; (d) BSA–picloram/picloram antibody modified electrode after incubation with HRP–G anti-RlgG. The frequency range was from 1 Hz to 100 kHz, whereas the amplitude of the alternating voltage was 5 mV. All measurements were performed in 10 mM PBS (pH 7.4) containing 0.1 M KCl and 5 mM $K_3[Fe(CN)_6]/K_4[Fe(CN)_6]$.

CV and chronoamperometry measurement were carried out to study the immunosensor electrochemical behaviors. From the CV curve, we can see that the immunosensor displayed a low background current without observable electrochemical response in blank PBS (pH 7.4) (Fig. 3, curve a). When hydroquinone and H_2O_2 were added, the electrochemical response showed an obvious increase of the reduction current and a negligible oxidation current (Fig. 3, curve b) that was attributed to the enzymatic catalysis of the immobilized HRP for the hydroquinone and H_2O_2 .

In the presence of H_2O_2 , the hydroquinone was first oxidized to quinone compounds by HRP. Then the quinone compounds were subsequently reduced at the electrode with an applied potential of -0.2 V versus SCE. Thus, a detectable current was generated.

Fig. 4 displays a typical current–time curve for the addition of 0, 0.5, and 2 μ g/ml picloram for the three electrodes at -0.2 V. We can see that when no picloram was present, the current is maximum (curve a). The current decreased when 0.5 and 2 μ g/ml picloram was added (curves b and c). Picloram would compete with BSA–picloram to combine picloram antibody, thereby reducing the amount of HRP–G anti-RlgG and causing the current decrease.

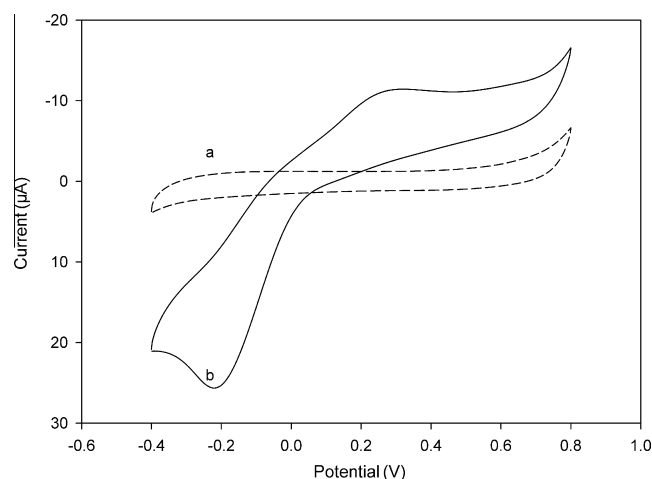


Fig. 3. Cyclic voltammograms of HRP–G anti-RlgG/antibody/BSA–picloram/Au nanocluster GCE in blank PBS (pH 7.4) (a), with the addition of 1 mM hydroquinone and 2 mM H_2O_2 (b), at 50 mV/s.

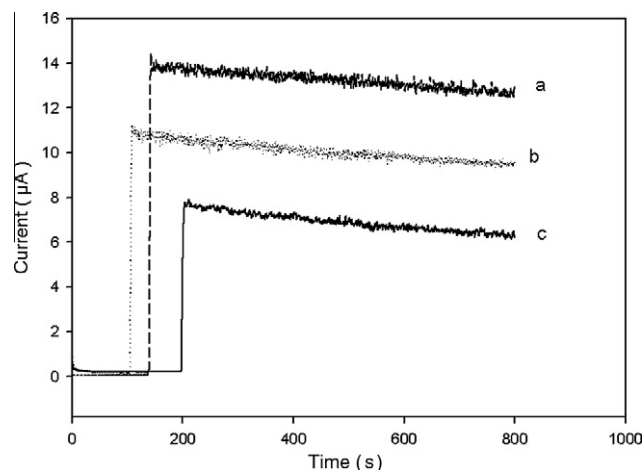


Fig. 4. Current–time curves of 0 μ g/ml picloram (a), 0.5 μ g/ml picloram (b), and 2 μ g/ml picloram (c). All measurements were performed in the presence of 1 mM hydroquinone and 2 mM H_2O_2 at -0.2 V under increasing stirring.

Optimization of measurement variables

The pH value of the detection solution is an important factor of the immunosensor performance. Most enzymes display good activity only in a limited pH range. Taking account of this factor, we investigated the pH influence of the immunosensor over the pH range of 4.6–8.5. The highest signal-to-background current was

detected in the pH range of 7.0–7.5. Therefore, the optimal current response was obtained in the pH range of 7.0–7.5. To achieve the maximum sensitivity, pH 7.4 was chosen in subsequent experiments and was also a general pH value in immunology (Fig. 5A).

The effect of hydroquinone concentration on the HRP electrode response was studied in the presence of excess H₂O₂. The response current increased sharply, with the hydroquinone concentration

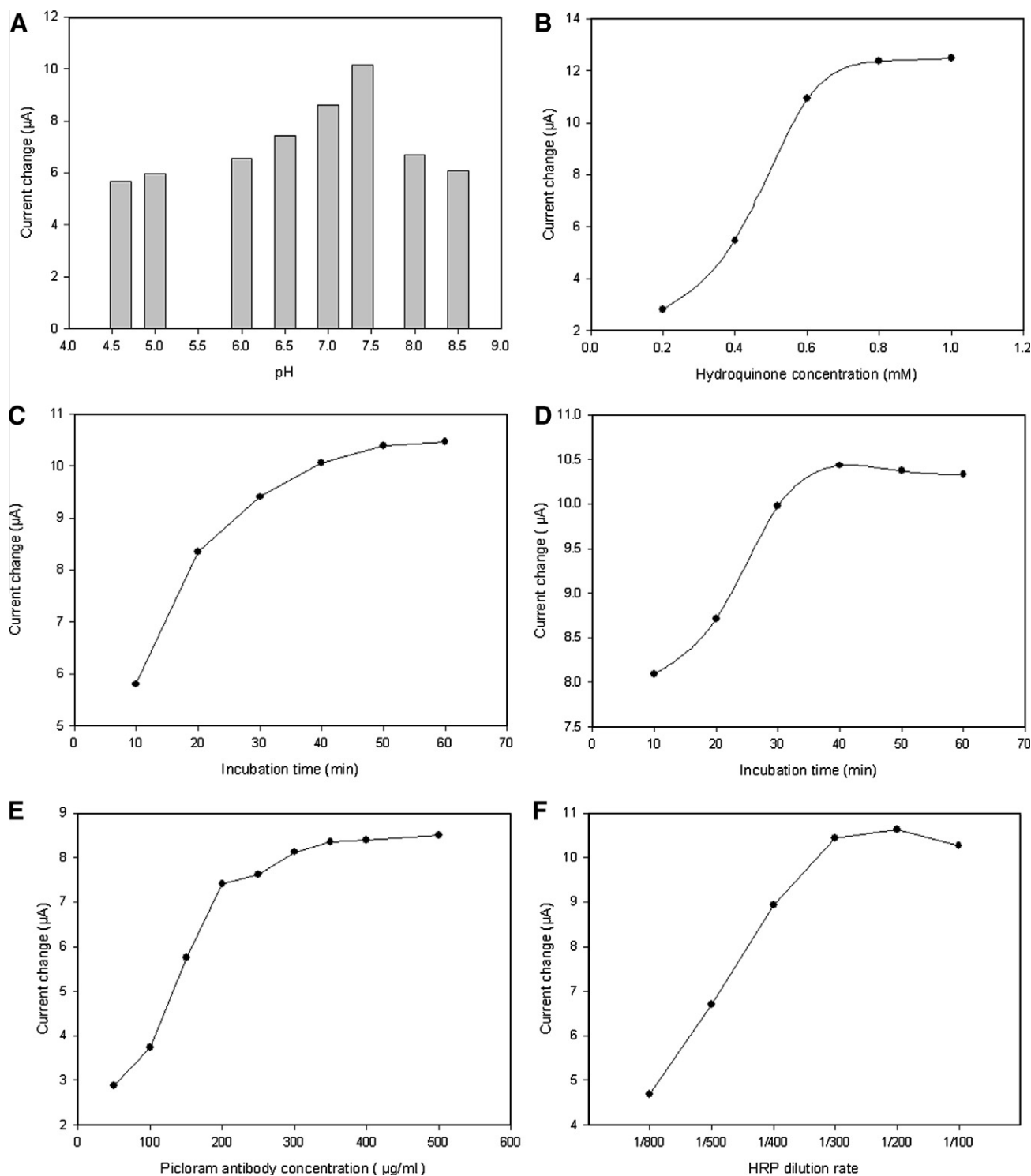


Fig. 5. (A) Effects of pH value of the detection solution on the current response of the immunosensor in PBS containing 1 mM hydroquinone and 2 mM H₂O₂. (B) Effects of hydroquinone concentrations on current response in PBS (pH 7.4) at optimized applied potential of -0.2 V. (C and D) Effects of incubation time for antibody (C) and HRP-G anti-RlgG (D) for immunoreaction with 300 µl of antibody at pH 7.4 on current response. (E) Dependence of current response of immunosensor on picloram antibody concentration in immunoreaction for 60 min at pH 7.4. (F) Optimization of dilution rate of HRP-G anti-RlgG under optimized conditions.

increasing from 0.2 to 0.6 mM and then leveling off (Fig. 5B). Therefore, 1 mM hydroquinone was used in further experiments. At this point, the concentration of H₂O₂ was investigated. The current response reached saturation at the concentration of 2 mM H₂O₂.

The influencing factors of immunoreaction were also investigated, including picloram antibody concentration and incubation time, dilution ratio, and incubation time of HRP-G anti-R1gG. The response current increased with the increasing incubation time and reached plateaus at 60 and 40 min for antibody incubation and HRP-G anti-R1gG incubation, respectively (Fig. 5C and D). The investigated picloram antibody concentrations ranged from 100 to 500 µg/ml. The response current reached the maximum at a concentration of 300 µg/ml (Fig. 5E). Therefore, 300 µg/ml picloram antibody was chosen as the optimized concentration. In addition, the optimal dilution rate of HRP-G anti-R1gG was 1:300 (Fig. 5F).

Response of the immunosensor to picloram concentration

Under the optimal immunoreaction and detection conditions, the target picloram molecules in sample solution would compete with the immobilized BSA–picloram to react with the limited molecules of dissociative picloram antibody to form immunocomplex. The current response decreased gradually with the increase of the concentration of target picloram (Fig. 6). The average decreasing percentage is linearly related to the natural logarithm of picloram concentration in the range from 0.001 to 10 µg/ml. The corresponding regression equation is

$$y = (2.778 \pm 0.3468)x + (30.76 \pm 1.998),$$

where y is the current decrease percentage, x is the natural logarithm of picloram concentration, and the correlation coefficient is 0.996. The lower LOD is 5.0×10^{-4} µg/ml, which resulted in a current signal that equals the mean value of background signals plus three times the standard deviation of background signals. The limit of quantification (LOQ) is 0.0021 µg/ml, which was obtained from $LOQ = 10(S_b/m)$, where S_b is the standard deviation of current measurements of the blank solution at the concentration range between 0.001 and 10 µg/ml and m is the slope of the analytical curve.

Each of the calibrations is conducted three times with the standard deviations of current response no more than 3.87%.

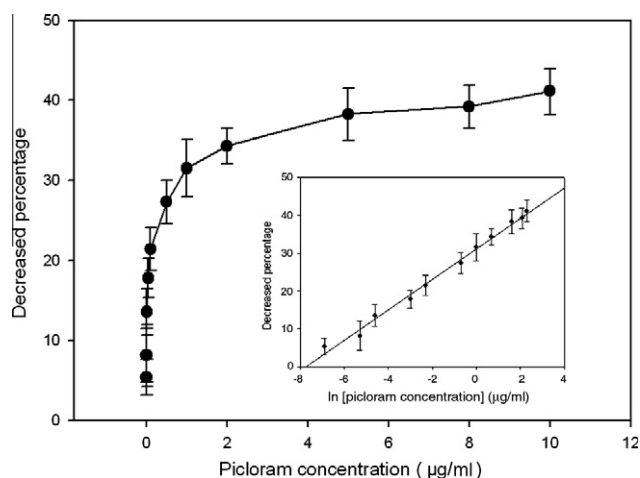


Fig. 6. Calibration curve of immunosensor for picloram determination under the optimal experimental conditions. Inset: Linear regression of decrease percentage versus the natural logarithm of picloram concentration. The vertical bars designate the standard deviations for the mean of three replicative tests.

The LOD is lower, and the linear range is larger, than in our previous work, and this may be attributed to three reasons. First, the formed chitosan film hinders the diffusion of electrons toward the electrode surface because of its relatively poor conductivity. Second, our previous work used the entrapment method to immobilize BSA–picloram, which is simple and convenient, but the entrapped randomly oriented biomolecules may lose bioactivities. In the current study, the BSA–picloram was combined with functional group. It is a better strategy to immobilize biomolecules for better biomolecules orientation and to increase the biomolecule density. Third, due to the large surface area of the special 3D structure, the proposed nanomaterial might be effective for the immobilization of biomolecules. It can combine a much greater number of biomolecules than the solid electrode. At the same time, there are spaces among columnar structures acting as an electron transfer channel, and the contact area with the electrolyte gets expanded, thereby promoting the electron transfer. That is why the LOD improves.

The LOD is smaller than those for the previously reported assay methods for picloram determination described in the introductory paragraphs of this article. We consider that a small LOQ is favored by good conductivity, good electron transfer ability, and large surface area. In addition, there are other weaknesses of previously described methods. For example, it is difficult to recover used Hg in the hanging mercury drop electrode method, and this will lead to environmental pollution. In addition, it involves extensive sample extraction and purification procedures and well-equipped laboratory installations in gas/liquid chromatography with electron capture detector and the capillary electrophoresis/mass spectrometry method.

Detection of picloram in samples

Picloram, which is usually used for prevention and control of the fruit moth class, red spider, white spider, and cabbage caterpillar, or the bollworm on vegetables, is easy to move and difficult to degrade. Peach extract and excess sludge supernatant were spiked with different concentration of picloram analyzed by the immunosensor. The results of the samples are shown in Table 1, which indicates that the immunosensor was a reliable determination method for picloram in the environmental samples.

Each detection was done three times, with the standard deviations of current response not being more than 9.24%.

Specificity of immunosensor

To evaluate the selectivity of the biosensor, some possible interfering substances, such as clopyralid, fluroxypyr methyl, quinclorac, and Iontrel, were examined under the same conditions for the picloram determination. From the results (Table 2), we could infer that the interference of these chemicals to the immunosensor

Table 1
Picloram concentration in peach and excess sludge supernatant determined by proposed immunosensor.

Sample	Concentration added (µg/ml)	Concentration found (µg/ml)	Recovery (%)	Relative signal deviation (%)
Peach	0.01	0.011 ± 0.003	110	4.19
	0.2	0.187 ± 0.063	93.5	9.24
	5	5.17 ± 0.37	103.4	5.77
Excess sludge supernatant	0.2	0.201 ± 0.006	100.5	6.03
	1	0.98 ± 0.42	98	2.11
	5	5.26 ± 0.89	105.2	7.37

Table 2

Comparison of the immunosensor response to picloram and other structurally related compounds under the same conditions.

Interferent	Concentration (μg/ml)	Decrease percentage of current (μA)	Current response (%)
Picloram	0.5	27.33	9.48
Clopyralid	0.5	4.61	12.45
Fluroxypyr methyl	0.5	2.39	13.12
Quinclorac	0.5	3.10	12.66
Lontrel	0.5	1.77	12.82

was negligible, although all of them contained the same pyridyl structure as that of picloram.

Stability and reusability

The performance stability of the immunosensor was examined. The Au nanoclusters modified GCE was stored at 4 °C when not in use. The current of the biosensor kept an invariable value for approximately 15 days with a negligible decrease. This observation indicated that the stability of this biosensor might be sufficient for practical applications. The bioactivity remained unchanged owing to biocompatibility in the microenvironment of Au nanocluster.

One of the concerns about the immunosensor is its reusability. The regeneration of the immunosensor was successively carried out in NaOH solution containing 0.5 M NaCl and in DMF. By this means, the immunocomplexes and the resultants of enzymatic catalytic reaction were released from the sensing surface and the regenerated Au nanoclusters modified electrode can be used to fabricate a new sensing interface. After that, the regenerated Au nanoclusters modified electrode could be used for the next detection. After regeneration, the response of the same sample was nearly the same as the original signal. Having been regenerated for five runs, 85% of the original current response was observed.

Conclusion

A picloram biosensor has been developed for detecting trace picloram in the environment on the basis of the immunoreaction. BSA–picloram, picloram antibody (competing with target picloram), and HRP-labeled secondary antibody were immobilized on the 3D Au nanoclusters modified GCE in turn. The optimized experimental conditions for the operation of the picloram biosensor were studied. The newly developed immunosensor based on Au nanoclusters possesses advantages such as simple fabrication, fast response, low LOD, wide linear range, easy regeneration, excellent reproducibility, and long stability. The relatively wide linear range and high sensitivity can be attributed to the electrodeposited Au nanoclusters with good biocompatibility, large specific surface area, and high electron exchange capability. All of these observations clearly illustrated that this immunosensor could be used for the on-site monitoring of trace picloram in environmental matrices in further studies.

Acknowledgments

This study was financially supported by the National Natural Science Foundation of China (50608029, 50978088, 51039001, and 50808073), the Special Fund for Basic Scientific Research of Central Colleges (Hunan University), the Hunan Key Scientific Research Project (2009FJ1010), the Hunan Provincial Natural Science Foundation of China (10JJ7005), and the Program for Changjiang Scholars and Innovative Research Team in University (IRT 0719).

Appendix A. Supplementary data

Supplementary data associated with this article can be found, in the online version, at doi:10.1016/j.ab.2010.08.001.

References

- [1] K. Borgå, T.F. Bidleman, Enantiomer fractions of organic chlorinated pesticides in arctic marine ice fauna, zooplankton, and benthos, *Environ. Sci. Technol.* 39 (2005) 3464–3473.
- [2] N. Pant, R. Kumar, N. Mathur, S.P. Srivastava, D.K. Saxena, V.R. Gujrati, Chlorinated pesticide concentration in semen of fertile and infertile men and correlation with sperm quality, *Environ. Toxicol. Pharmacol.* 23 (2007) 135–139.
- [3] D.J. Lee, S.A. Senseman, A.S. Sciombato, S.C. Jung, L.J. Krutz, The effect of titanium dioxide alumina beads on the photocatalytic degradation of picloram in water, *J. Agric. Food Chem.* 51 (2003) 2659–2664.
- [4] R. Grover, A.J. Cessna, *Environmental Chemistry of Herbicides*, vol. 1, CRC Press, Boca Raton, FL, 1988.
- [5] J.F. Fairchild, K.P. Feltz, L.C. Sappington, A.L. Allert, K.J. Nelson, J. Valle, An ecological risk assessment of the acute and chronic toxicity of the herbicide picloram to the threatened bull trout (*Salvelinus confluentus*) and the rainbow trout (*Oncorhynchus mykiss*), *Arch. Environ. Contam. Toxicol.* 56 (2009) 761–769.
- [6] A. Ghauch, Degradation of benomyl, picloram, and dicamba in conical apparatus by zero-valent iron powder, *Chemosphere* 43 (2002) 1109–1117.
- [7] M.R.C. Massaroppi, S.A.S. Machado, L.A. Avaca, Electroanalytical determination of the herbicide picloram in natural waters by square wave voltammetry, *J. Braz. Chem. Soc.* 14 (2003) 113–119.
- [8] U.S. Environmental Protection Agency, *Drinking Water Advisory: Pesticides*, second ed., Lewis, Chelsea, MN, 1991, p. 819.
- [9] L.B.O. Santos, J.C. Masini, Determination of picloram in natural waters employing sequential injection square wave voltammetry using the hanging mercury drop electrode, *Talanta* 72 (2007) 1023–1029.
- [10] R. Rodríguez, J. Mañes, Y. Picó, Off-line solid-phase microextraction and capillary electrophoresis mass spectrometry to determine acidic pesticides in fruits, *Anal. Chem.* 75 (2003) 452–459.
- [11] K.Y.F. Yau, N.L. Tout, J.T. Trevors, H. Lee, J.C. Hall, Bacterial expression and characterization of a picloram-specific recombinant Fab for residue analysis, *J. Agric. Food Chem.* 46 (1998) 4457–4463.
- [12] K.Y.F. Yau, M.A.T. Groves, S. Li, C. Sheedy, H. Lee, J. Tanha, C.R. MacKenzie, L. Jermutus, J.C. Hall, Selection of hapten-specific single-domain antibodies from a non-immunized llama ribosome display library, *J. Immunol. Methods* 281 (2003) 161–175.
- [13] J.C. Hall, R.J.A. Deschamps, K.K. Krieg, Immunoassays for the detection of 2,4-D and picloram in river water and urine, *J. Agric. Food Chem.* 37 (1989) 981–984.
- [14] T.R. Glass, N. Ohmura, Y. Taemi, T. Joh, Simple immunoassay for detection of PCBs in transformer oil, *Environ. Sci. Technol.* 39 (2005) 5005–5009.
- [15] S.Y. Rabbany, W.J. Lane, W.A. Marganski, A.W. Kusterbeck, F.S. Ligler, Trace detection of explosives using a membrane-based displacement immunoassay, *J. Immunol. Methods* 246 (2000) 69–77.
- [16] L. Tang, G.M. Zeng, G.L. Shen, Y.P. Li, Y. Zhang, D.L. Huang, Rapid detection of picloram in agricultural field samples using a disposable immunomembrane-based electrochemical sensor, *Environ. Sci. Technol.* 42 (2008) 1207–1212.
- [17] Y. Zhang, G.M. Zeng, L. Tang, D.L. Huang, X.Y. Jiang, Y.N. Chen, A hydroquinone biosensor using modified core-shell magnetic nanoparticles supported on carbon paste electrode, *Biosens. Bioelectron.* 22 (2007) 2121–2126.
- [18] L. Tang, G.M. Zeng, J.X. Liu, X.M. Xu, Y. Zhang, G.L. Shen, Y.P. Li, C. Liu, Catechol determination in compost bioremediation using a laccase sensor and artificial neural networks, *Anal. Bioanal. Chem.* 391 (2008) 679–685.
- [19] S. Upadhyay, G.R. Rao, M.K. Sharma, B.K. Bhattacharya, V.K. Rao, R. Vijayaraghavan, Immobilization of acetylcholinesterase–choline oxidase on a gold–platinum bimetallic nanoparticles modified glassy carbon electrode for the sensitive detection of organophosphate pesticides, carbamates, and nerve agents, *Biosens. Bioelectron.* 25 (2009) 832–838.
- [20] B. Girginer, G. Galli, E. Chiellini, N. Bicak, Preparation of stable CdS nanoparticles in aqueous medium and their hydrogen generation efficiencies in photolysis of water, *Int. J. Hydrogen Energy* 34 (2009) 1176–1184.
- [21] Z. Khan, S.A. Al-Tnabaiti, E.H. El-Mossalamy, A.Y. Obaid, Effect of macromolecule poly(vinyl alcohol) on the growth of cetyltrimethylammonium bromide stabilized Ag nanoparticles, *Colloids Surf. A* 352 (2009) 31–37.
- [22] S. Thiagarajan, R.F. Yang, S.M. Chen, Palladium nanoparticles modified electrode for the selective detection of catecholamine neurotransmitters in presence of ascorbic acid, *Bioelectrochemistry* 75 (2009) 163–169.
- [23] H. Araki, A. Fukuoka, Y. Sakamoto, S. Inagaki, N. Sugimoto, Y. Fukushima, M. Ichikawa, Template synthesis and characterization of gold nano-wires and -particles in mesoporous channels of FSM-16, *J. Mol. Catal. A* 199 (2003) 95–102.
- [24] S. Thangavel, R. Ramaraj, Polymer membrane stabilized gold nanostructures modified electrode and its application in nitric oxide detection, *J. Phys. Chem. C* 112 (2008) 19825–19830.
- [25] L. Tang, G.M. Zeng, G.L. Shen, Y. Zhang, Y.P. Li, C.Z. Fan, C. Liu, C.G. Niu, Highly sensitive sensor for detection of NADH based on catalytic growth of Au

- nanoparticles on glassy carbon electrode, *Anal. Bioanal. Chem.* 393 (2009) 1677–1684.
- [26] M.H. Yang, F.L. Qu, Y.J. Li, Y. He, G.L. Shen, R.Q. Yu, Direct electrochemistry of hemoglobin in gold nanowire array, *Biosens. Bioelectron.* 23 (2007) 414–420.
- [27] A. Ambrosi, M.T. Castañeda, A.J. Killard, M.R. Smyth, S. Alegret, A. Merkoci, Double-codified gold nanolabels for enhanced immunoanalysis, *Anal. Chem.* 79 (2007) 5232–5240.
- [28] S. Isik, L. Berdondini, J. Oni, A. Blochl, M. Koudelka-Hep, W. Schuhmann, Cell-compatible array of three-dimensional tip electrodes for the detection of nitric oxide release, *Biosens. Bioelectron.* 20 (2007) 1566–1572.
- [29] B. Erdogan, L. Song, J.N. Wilson, J.O. Park, M. Srinivasarao, U.H. Bunz, Permanent bubble arrays from a cross-linked poly(*para*-phenyleneethynylene): picoliter holes without microfabrication, *J. Am. Chem. Soc.* 126 (2004) 3678–3679.
- [30] L.T. Qu, G.Q. Shi, F.E. Chen, J.X. Zhang, Electrochemical growth of polypyrrole microcontainers, *Macromolecules* 36 (2003) 1063–1067.
- [31] M.A. Correa-Duarte, N. Wagner, J. Rojas-Chapana, C. Morsczeck, M. Thie, M. Giersig, Fabrication and biocompatibility of carbon nanotube-based 3D networks as scaffolds for cell seeding and growth, *Nano Lett.* 4 (2004) 2233–2236.
- [32] H. Hu, Y.C. Ni, V. Montana, R.C. Haddon, V. Parpura, Chemically functionalized carbon nanotubes as substrates for neuronal growth, *Nano Lett.* 4 (2003) 507–511.
- [33] S.P. Wang, Z.S. Wu, F.L. Qu, S.B. Zhang, G.L. Shen, R.Q. Yu, A novel electrochemical immunosensor based on ordered Au nano-prickle clusters, *Biosens. Bioelectron.* 24 (2008) 1026–1032.